PHYSICAL REVIEW E **109**, 014607 (2024)

Featured in Physics

Formation and mechanics of fire ant rafts as an active self-healing membrane

Chung-Hao Chen,[1] Ting-Heng Hsieh,[1] Hong-Yue Huang,[1] Yu-Chuan Cheng,[1,2] and Tzay-Ming Hong[1,*]
[1]*Department of Physics, National Tsing Hua University, Hsinchu, Taiwan 30013, Republic of China*
[2]*Department of Physics, University of California at Santa Barbara, Santa Barbara, California 93106, USA*

(Received 2 July 2023; accepted 16 November 2023; published 9 January 2024)

The unique ability of fire ants to form a raft to survive flooding rain has enchanted biologists as well as researchers in other disciplines. It was established during the last decade that a three-dimensional aggregation of fire ants exhibits viscoelasticity with respect to external compression and shearing among numerous unusual mechanical properties. Continuing these works, we will study the ant raft in its natural form, i.e., composing no more than two layers. This allowed us to focus on the cracks that are unique to membranes and see how their patterns are influenced by the fact that these ants are mobile and can self-repair the damage to keep their raft from disintegration. In the beginning, we show that vertical and horizontal shaking can also prompt fire ants to aggregate. The canonical view that the stability of ant raft relies on the Cheerios effect and a combination of other parameters is tested. The force-displacement experiment is performed to show that two distinct mechanical responses and fracture patterns, characteristic of ductile and brittle materials, can be elicited, depending on the magnitude of the pull speed. During the process, we counted the number of ants that actively participated in the stress-strain relation and used this information to roughly sketch out the force chain. The latter information reveals that the pull force expedites the alignment of fire ants, in analogy to the effect of an electric field on liquid crystal polymers. To highlight the self-healing nature, we employ the creep experiment to study how the length and Young's modulus of the raft change or relax with time. One major finding is that the raft can exhibit zero Poisson's ratio without resorting to specific geometry structures. This is enabled by the active recruitment of ants from the top layer to the bottom layer to keep the raft from disintegrating.

DOI: 10.1103/PhysRevE.109.014607

I. INTRODUCTION

Examples of collective behavior, shaped by a hundred million years of evolution to adapt to the changing environments, are ubiquitous in the animal kingdom, and include bird flocking [1,2], cell motion [3], and bacterial growth [4]. How these individuals can mediate internal interactions in order to display an intelligent emerging response despite the lack of a centralized system has enthralled scientists as well as engineers. One recent development in bionics is to synthesize materials that exhibit similar emergent phenomena, like Janus particles [5,6], robots with local sensing [7] and microtubule-based liquid crystal [8]. This inclination to socialize and collaborate makes sense particularly for the tiny ants to bring back a large insect or fight off an invading enemy. Moreover, some species of ants develop the skill to aggregate and form a thread to cross a gap or to reach higher ground. In the last 80 years or so, fire ants have attracted much attention not only because their global invasion causes agricultural losses, medical treatments, and damage to properties annually in the USA [9], but also for academic reasons. The latter has to do with their unique ability to form rafts in order to float and survive flooding [10]. This has captivated the imagination of material engineers and physicists who already succeeded at characterizing their viscoelastic and other distinct mechanical properties in the form of a raft or bulk [11–15].

The main theme of this work is to study the mechanical properties of an ant raft as a quasi-two-dimensional material with the focus on which properties descend from the fact that these ants are alive and capable of moving and mending their raft. Before entering the core study, we would like to add some thoughts to the canonical view on how the ant raft is formed. Hu *et al.* [16,17] proposed that the Cheerios effect [18], i.e., the surface tension, is crucial to the stability of rafts that is also influenced by a combination of parameters, such as the active force of individual ants and the initial spacing between them. They numerically simulated the ants repelling each other due to panic, and it was only after the water was taken into account that their aggregation became possible. However, a large crowd, roughly exceeding seven, was found to be necessary to stabilize the raft [17]. The clumping of cereals that float in our bowl of milk at breakfast apparently attests to the correctness of their explanation. However, why did this ability to form a raft on water not also exist in other species of ants or recently deceased fire ants? Not directly related to their model, another question can be whether the Cheerios effect is necessary, namely, is the medium of water necessary to trigger the formation of a raft? To answer these queries, we arranged to experiment on live and dead fire ants and a different species of ant, and also put them on a shaker to test if a crisis can prompt the action of aggregation. Rafts formed by different means are distinguished by their morphology and how fast it takes for the ants to assemble and how long to dissolve after the raft is allocated to a solid surface.

---

[*] ming@phys.nthu.edu.tw

Continuing the work by Tennenbaum *et al.* [11] who studied the viscoelastic and fluidlike properties by oscillating and rotating three-dimensional (3D) fire ant aggregates, we pay attention to the 2D ant raft formed on water and perform a uniaxial tensile test and linear creep experiment to search for new characteristics driven by active and self-healing nature. They include measuring the responses at different pull speeds, such as the resistance force, crack modes, and Young's modulus during relaxation, and then comparing them with the common tissue and bubble raft [19–27] to accentuate the effect when the constituents cannot only actively adjust their position and role in response to external forces, but also possess healing power. This information is valuable since, although the literature abounds for either active or self-healing material [28–33], their combination is rare.

Bear in mind that material failure is usually classified into brittle [34–36] and ductile [16,37–39], where the former has nearly no plastic deformation and breaks down like an avalanche at the macroscopic scale. In contrast, the fracture processes in a ductile material are more complex so that holes appear randomly on the film and eventually cause fracture upon extension. A similar comparison has been made to the fire ant raft by concentrating on viscoelasticity and activeness. Besides elaborating on these macroscopic properties, we zoom in on each ant and analyze how the force chain develops and propagates with the pull force and relaxation time. The structure of the force chain is hard to determine and has only been studied in granular material [40,41] because its constituents are constantly in a jammed state without external vibrations. The Janssen effect, observed for a fire-ant column by measuring its apparent mass [42], indirectly confirmed the existence of a force chain but failed to provide any information on its dynamics.

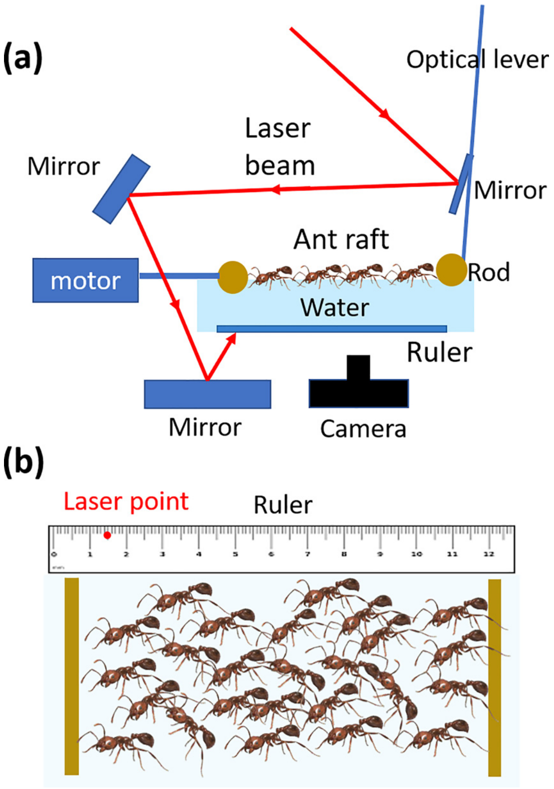

FIG. 1. (a) Schematic experimental setup for measuring the mechanical and creep properties of fire ant rafts. (b) The displacement of the laser point on the ruler allows us to determine the bending angle of the optical lever and hence the resistance force of ants from this bottom view of (a).

II. EXPERIMENTAL SETUP

Our samples consist of fire ants (*Solenopsis invicta*) and a common species (*Monomorium chinense*) in Taiwan, both of which are approximately 5 mm in length. We adopted the methods used by Chen [43] to retrieve ants from the field and separate them from the soil. Once separated and placed into a plaster nest, ants are fed with sugar, crickets, and water. To measure the resistance force F of ants as we pull the raft, a

TABLE I. Side and top views of fire ants, local ants, and dead fire ants under different environments to facilitate aggregation.

	on water	vertical shaking	horizontal shaking
fire ants	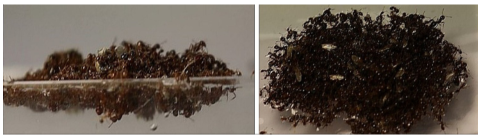		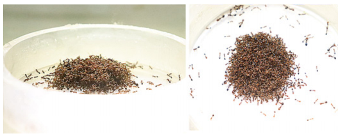
local ants		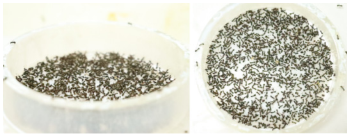	
dead ants	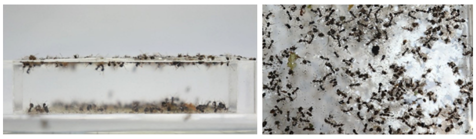	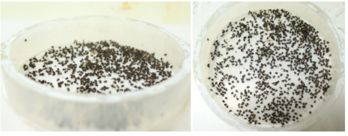	

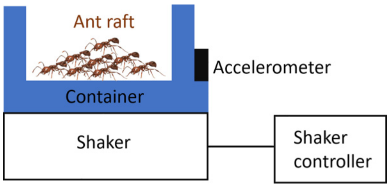

FIG. 2. A shaker is employed to test whether flooding is the only means to induce the action of aggregation for fire ants. Note that ants never touch the wall when jiggled horizontally. The container is coated with Teflon (Chemours DISP 30) to prevent fire ants from gripping and escaping.

homemade force sensor was designed with an optical lever [44], as shown in Fig. 1. Note that the worker ants would gather around to protect the queen ants, which results in a raft with uneven thickness and comprising more than four layers, as shown in Table I. Our protocol is to always remove the queen ants from the raft before the experiment to achieve a more even double-layer structure. For the ants to cling to, two wooden rods of diameter = 1 cm are arranged on both sides of the raft. While one rod is fixed to the lever, the other is pulled by a motor at a constant speed v. The optical lever consists of a mirror and a thin glass fiber of length 50 cm and diameter 0.1 cm. The morphology of the ant raft is video recorded simultaneously with the resistance force. In addition, the number of ants at the bottom layer, which is mostly static and believed to compose the raft and contribute to countering F, and their orientation are determined by image processing. To test whether aggregation can be induced by means other than flooding, we bring into action the shaker in Fig. 2 with the frequency range 35–55 Hz and root-mean-square acceleration 1–3 g, where $g = 9.8\ \mathrm{m/s^2}$. It is enabled by an accelerometer and is switchable between vertical and horizontal modes.

III. EXPERIMENTAL RESULTS

A. Raft formed by different means

By tuning the frequency and amplitude of the shaker in Fig. 1(b), we can simulate a zero-gravity environment. As shown in Table I, local ants and dead fire ants remain scattered on water, while live fire ants aggregate under both vertical and horizontal shaking. First, the failure of local ants to form a raft on the water can be explained by the active repulsive force exerted by individual ants on their neighbors, as foreseen by Ref. [17]. Second, the equally unsuccessful observation of raft for recently deceased fire ants [45] can also be ascribed to the lack of a close spacing between ants due to the spread out of their limbs. The shaker experiment serves to demonstrate that, while the model in Ref. [17] remains correct, the urge to assemble and form an aggregate when facing an existential crisis is triggered by something more general than the Cheerios effect.

The vertical shaking generates a ball-like structure, conspicuously different from the double-deck raft on the water. This is in contrast to the pancakelike aggregate triggered by horizontal shaking. No raft formation is seen for local ants in all three circumstances, likely due to the repulsion from their vigorous waving of legs. In addition to morphology, aggregates of ants formed by different means can also be distinguished by the time it takes for the ants to accumulate or disperse after the cluster is relocated to safe and firm ground, as compiled in Table II. Unlike water on which ants can float and survive for dozens of minutes, shaking is an imminent danger that calls for immediate action and thus leads to a shorter aggregation time. But why is the relaxation time more than twice the aggregation time? The Cheerios effect is not a good candidate to explain this because the ant raft was put on a plaster plate whose porous structure can quickly absorb the water that remains in the raft. Furthermore, had there been any water that glues and keeps ants from dispersing, those ants ought to have shown signs of struggling, but in fact they were pretty much motionless. Based on the theory by Wilson and his coworkers [46] that pheromones are essential for communication among ants, we conjecture that the relaxation time is constrained by the diffusion process for the pheromone(s), the messenger that calls on the fire ants to aggregate in times of danger, to disperse so that the intoxicated ants can finally sober up and disseminate. In the meantime, it goes without saying why the dead ant raft never relaxes.

B. Force-displacement experiment

Since the membrane formed by plastic balls in Ref. [47] is also triggered by the Cheerios effect, we initially thought that the ant raft would exhibit similar properties under a linear extension. However, it turns out that they are very different. In essence, the aggregate of plastic balls behaves like a liquid drop with an effective surface tension endowed by the Cheerios effect. As a result, only a fast pull speed v can bring about a strong enough drag force to change its morphology. In contrast, the fire ant raft is readily susceptible to a low v, as demonstrated by the stress-strain curve in Fig. 3 for $v = 0.25$ mm/s, and can be separated into elastic, plastic, and rupture regions, denoted respectively as Reg. I, II, and III. Region II is characterized by the appearance of stationary cracks, first in the interior and then at the edge of the ant raft. These cracks start to expand irreparably upon entering region III before eventually breaking into two pieces at some critical raft length that decreases as v is raised. It is worth mentioning that no hole was observed to develop in the interior of the ant raft if the pulling speed was lower than 0.1 mm/s. In other words, the ant raft transits directly from region I to III over time. We believe this somewhat monotonic behavior can be ascribed to the self-heal characteristic of fire ants that, given ample time, they are able to repair the cracks before they deteriorate into holes. Videos can be found in the Supplemental Material [49].

The plastic region II is lacking as we switch to a high speed $v = 1.7$ mm/s, reminiscent of brittle material. Again, similarly to normal substances, the maximum resistance force is enhanced when pulled faster [50]. In contrast to other factors that cause the ductile to brittle transition, such as temperature [51], load, strength, and stress concentration, the sensitive dependence on the stress rate of the ant raft is reminiscent of non-Newtonian liquids, such as oobleck, that exhibit both viscous and elastic characteristics. This is consistent with the conclusion reached by applying oscillatory rheology to 3D fire ant aggregates [11]. In addition to the insightful discussions in Ref. [11], a successful statistical mechanics model for this

TABLE II. The characteristic aggregation and relaxation time for ant rafts formed on water and by vertical and horizontal shaking. In the beginning, 500 ants are randomly scattered, and the aggregation time is defined as the time it takes for half of the ants to cling together. The relaxation time measures how long it takes for the raft to disintegrate after being relocated to a stationary solid surface. An "X" means that the ants fail to aggregate. A star (⋆) indicates amplitude = 0.25 mm and frequency = 50 Hz.

	Aggregation time			Relaxation time		
	On water	Vertical shaking⋆	Horizontal shaking⋆	On water	Vertical shaking	Horizontal shaking
Fire ants	30 s	5 s	3 s	60 s	10 s	30 s
Local ants	X	X	X	X	X	X
Dead fire ants	X	X	1 s	X	X	∞

setup can be found in Ref. [13]. None of these properties are observed in the aggregate of plastic balls on water [47]. In addition to mechanical and morphological descriptions, we also paid attention to the detailed alignment of ants by taking photos of the raft from below. The ants on the top layer walk about freely and do not actively contribute to F and the raft formation [52], but are important as a reserve to drop down to become part of the structural bottom layer over a period of hours. Aided by image processing and comparing successive photos in time, we single them out when counting the active-duty ants at the bottom layer. Among them, those with orientation within 20° from the pull direction are tallied as number N and marked by red lines, otherwise they are in green. The degree of alignment is shown in Fig. 4 to correlate positively with the pull force, in analogy to a liquid crystal under an external electric field. The correlation is stronger in Fig. 4(a) than 4(b), presumably due to the ample time allowed by the low pull speed for ants to readjust their position to counter the applied force.

How does one extract some information about the structure of force chains from Fig. 4? Although the red lines already exist when the orientation of ants is supposed to be random at $F = 0$ from Fig. 4, we expect them to appear arbitrarily in space. Therefore, by paying attention to only those that are nearest neighbors, we can eliminate the randomness and identify the ants that actually contribute to the force chains. These pairs of red lines from Fig. 4(a) are replaced by blue ones. The reason why the blue lines are patchy in Fig. 5(a) for region I is that not all ants participating in the force chain are necessarily aligned to the force direction. Although only a partial force structure is glimpsed, Figs. 5(b) and 5(c) show that more and more ants on the force chain are aligned after entering regions II and III.

C. Creep experiment

The fact that its constituting members are active and capable of self-healing allows us to treat the fire ant raft as a novel membrane. In order to elucidate the effect of these characteristics on the material properties, we perform the creep experiment. As shown in Fig. 6, a region-I raft can relax to regions II and III over time, even for samples prepared by fast pull speed which originally lacks region II. Although no crack appears throughout region I, L is found to increase with time, while the width and height of the raft remain roughly constant. This implies a zero Poisson's ratio. Such a property is made

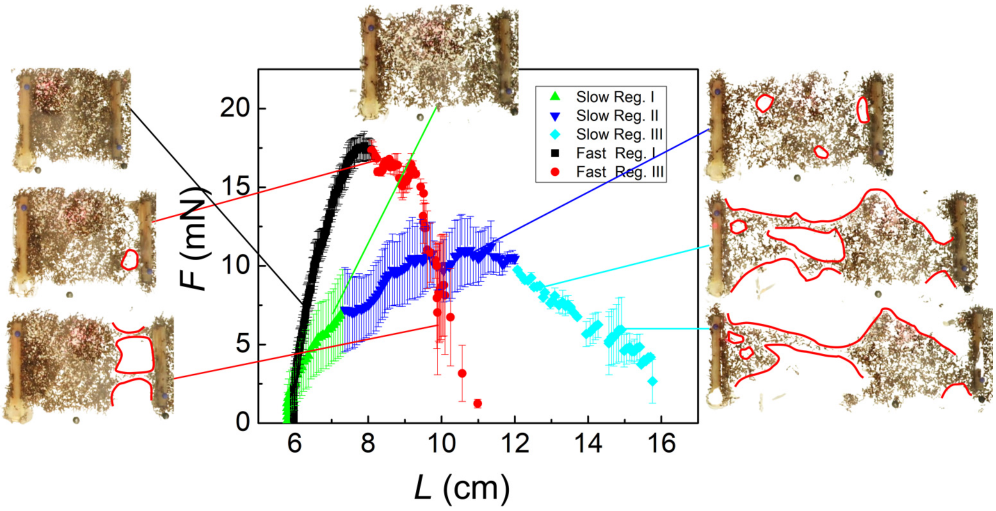

FIG. 3. The pull force versus length of ant raft under fast (1.7 mm/s) and slow (0.25 mm/s) pull speeds. Representative snapshots for each region are shown, where red curves are used to highlight the cracks that developed in the interior and at the edge of the ant raft. In contrast to being stationary in region II, these cracks expand irreversibly upon entering region III. Regions I, II, and III show the elastic, plastic, and rupture behaviors common to ductile materials [48]. The data for high pull speed are characterized as being brittle due to its lack of region II. The larger error bars for slow pulling are likely due to the fact that the ants are mobile, which accumulates more errors when given a longer time duration.

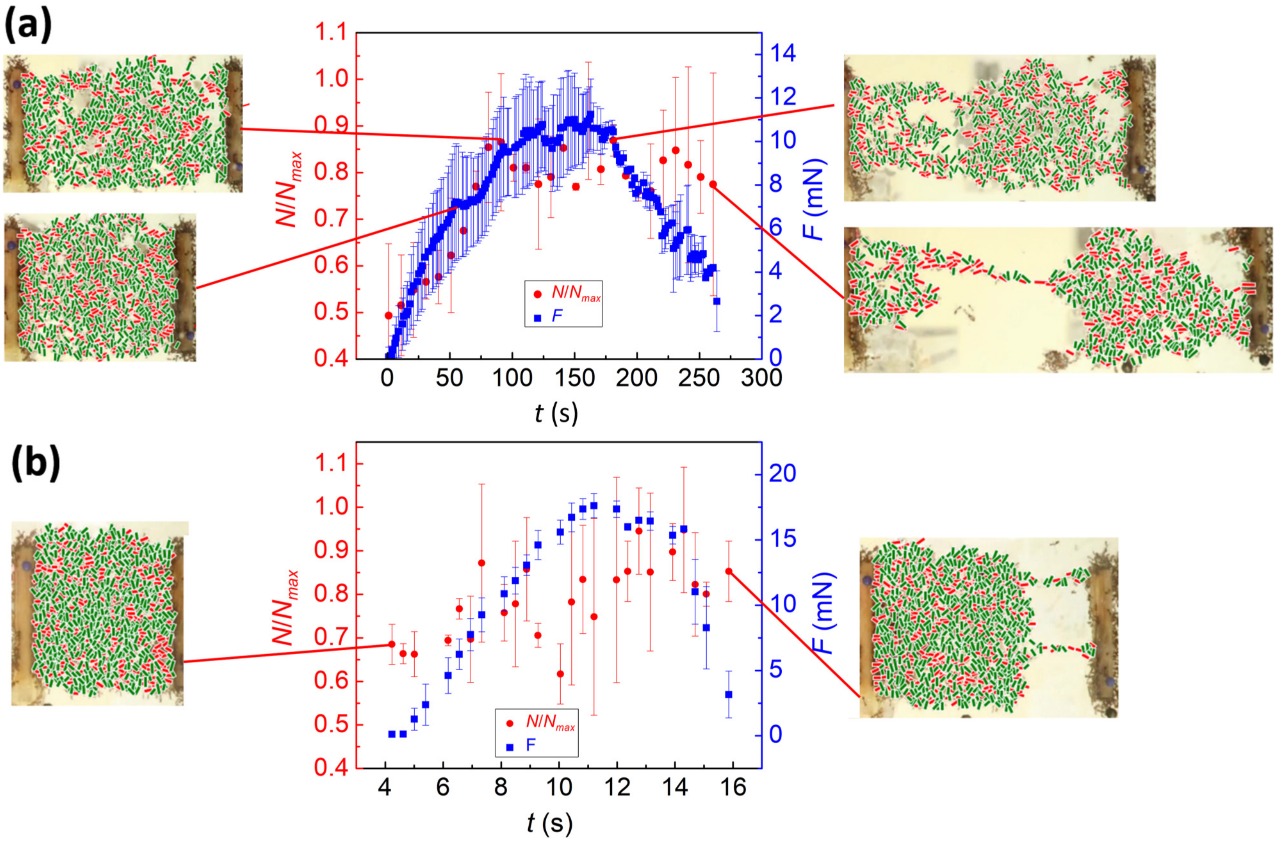

FIG. 4. In order to capture how the number of aligned ants N is correlated with the pull force F, they are plotted in double y-axis graphs as a function of time. Both quantities are rescaled by their maximum value to facilitate comparison. (a) and (b) are respectively for low and high pull speed. Alignment is defined by a deviation less than 20° between the ant orientation and the pull direction. These ants are marked by red lines in the photos, otherwise they are in green.

possible by the active movement of ants from the top layer to the bottom layer [15], presumably to help reinforce and keep the raft intact. As the raft runs out of ants on the top layer, two things happen as it enters region II: the raft area A begins to saturate and cracks start to develop. The latter weakens the structure of the raft and gives rise to a steeper slope in Fig. 6. Note that this is opposite to the behavior of most ductile materials where plastic deformation, movements, and generation of dislocation to be specific, strengthening the metal or polymer via work hardening. Since the region-III raft by a fast pull speed is very unstable, we only experiment on the sample prepared by a slow one. By definition, the existing

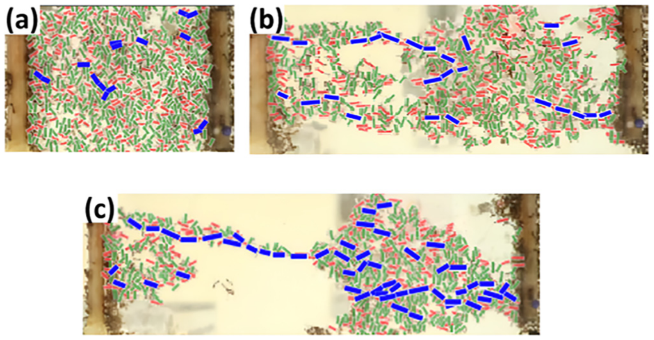

FIG. 5. Visualized by connecting the blue lines as defined in the text, force chains gradually develop from regions I and II in (a) and (b) to III in (c) for low pull speed.

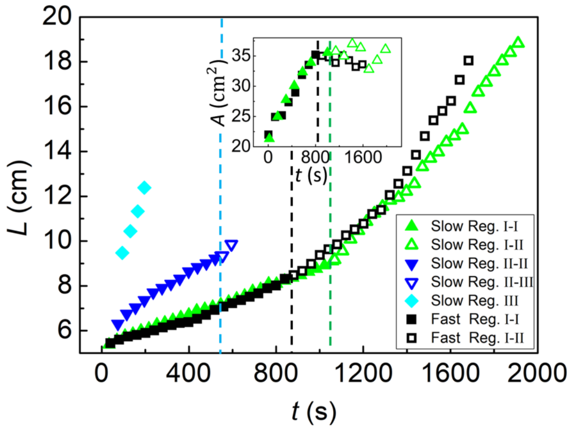

FIG. 6. Length L of the ant raft relaxes under a constant $F = 2.46$, 13.43, and 8.93 mN for Slow Reg. I, II, and III, and 3.4 mN for Fast Reg. I. The blue dashed line denotes the transition for Slow Reg. II-III data, i.e., for a slow pull speed, and from region II to III, when the ant raft ruptures irreversibly. Likewise, black is for Fast Reg. I-II, and green is for Slow Reg. I-II for holes appearing in the ant raft. The inset shows that the change of morphology for yellow and red lines is accompanied by an approximate saturation of raft area A.

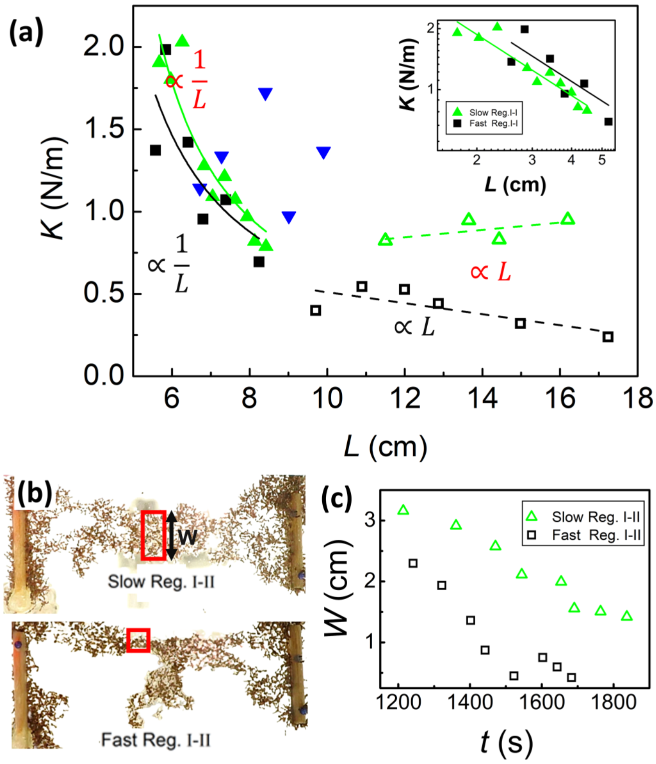

FIG. 7. (a) K vs L for the same samples in Fig. 6. Except for Slow Reg. II-II, the other four data are fitted respectively by solid ($1/L$) and dashed (L) green lines for slow speed, and the same in black for fast speed. The inset shows the log-log plot for Slow and Fast Reg. I-I that can be fit by the linear line. Although roughly observing the increasing trend as Slow Reg. I-II, the data of Slow Reg. II-II fluctuate wildly because we are forced to adopt a smaller ΔF to avoid hastening the raft into region III. This increases the uncertainty in ΔL. Snapshots of Slow and Fast Reg. I-II at $t = 1600$ s are shown in (b) where the primary neck, the one with the smallest width W, is identified and highlighted by the red rectangular box. (c) The W for the Fast Reg. I-II sample is not only narrower than that of Slow Reg. I-II, but also shrinks faster.

cracks start to expand irreversibly in this region, which thus renders an even larger dL/dt than that of region II in Fig. 6.

Equivalent to Young's modulus, an effective spring constant for the ant raft is defined as $K \equiv \Delta F/\Delta L$, where ΔL is the slight displacement to achieve a destined increment of resistance force ΔF during creeping. According to Fig. 7(a), their relationship changes as the raft prepared by slow pull transits from region I to II. If each ant behaves like a spring, we expect $K \propto W/L$ since the width W of the raft measures the number in parallel, while L is in series. Therefore, $K \propto 1/L$ is expected since W remains constant in region I. Entering region II, the shift to an increasing $K \propto L$ behavior perhaps reflects a desperate effort by the ants to strengthen their hold to prevent the raft from disintegrating. Now let us proceed and examine the fast pull data. The $K \propto 1/L$ in Fast Reg. I-I can be understood by the same argument as in Slow Reg. I-I. However, the higher rate of deterioration for the raft as one entity in Fast Reg. I-II than that in Slow Reg. I-II renders an opposite behavior. The neck in the former case is not only narrower, but its width also shrinks faster, as demonstrated by Figs. 7(b) and 7(c). We believe both factors bring about a shorter timescale than the reaction time for the ants to strengthen their spring constant, which results in a decreasing K with L, rather than increasing as in Slow Reg. I-II.

IV. CONCLUSION AND DISCUSSIONS

In support of the canonical view that the Cheerios effect is crucial to the stability of ant rafts, we tested on the inability for local ants and dead fire ants to aggregate on water. By demonstrating that fire ants can also be enticed to form an assemblage when subject to a vertical or horizontal shaking, we are inclined to side with the speculation by Wilson and argue that such an attractive behavior is likely triggered by some special pheromone when fire ants sense danger.

Two key ingredients distinguish the ant raft from sheets made of normal material. The first is activity: The fire ants are constantly moving, so their set of nearest neighbors is constantly changing. The second is the urge to mend and maintain the integrity of the raft. Insects take time to react to external stimuli and what their neighbors are doing, which sets an intrinsic response time. As a result, we found in the force-displacement experiment that (1) the stress-strain relationship at low pull speeds is similar to that of most ductile material, i.e., consisting of elastic, plastic, and rupture regions; (2) the plastic region shortens and the raft becomes more brittle-like as pull speed increases; (3) in analogy to the effect of an electric field on liquid crystal, the number of ants whose orientation is aligned to the pull force is positively correlated

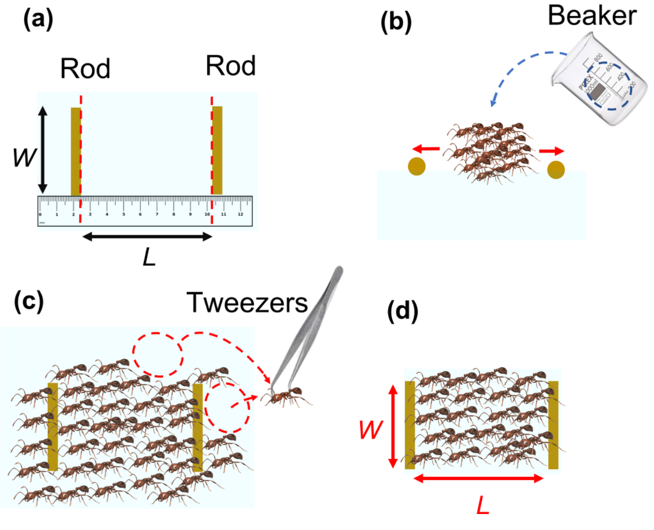

FIG. 8. Procedures for tailoring the width W and length L of an ant raft. (a) tTwo rods separated by a distance L with the aid of a ruler underwater. (b) After being gently deposited on water, the ball-shaped ants spread out and grip the rods. (c) A tweezer is used to remove the ants that exceed the designed range of W and L into the eventual raft sample in (d).

with the magnitude of the pull force; (4) the force chains can be mapped for regions II and III.

Furthermore, we found in the creep experiment that (5) the ant raft exhibits zero Poisson ratio, which is beneficial in the engineering of artificial cartilage, ligament, and cornea, for region-I samples, irrespective of their pull speed. Without relying on specific geometry structures, the ants manage such a feat by relocating their idle reserve from the top to the bottom layer to prevent the raft from disintegrating. In other words, the zero Poisson ratio is made possible by the fact that fire ants are alive and have the instinct to maintain the integrity of the raft. (6) The effective Young's modulus $\propto 1/L$ can be understood by the spring-network model in region I when the width of the raft is insensitive to extra stress.

Biomimicry is the emulation of the models, systems, and elements of nature for the purpose of solving complex human problems. Our study of fire ant raft as an active self-heal membrane reveals several interesting mechanical properties, such as zero Poisson's ratio and an effective Young's modulus that can be tailored to be proportional to the length of the ant raft or its inverse.

Recently, we became aware of a preprint [53] by Wagner *et al.* also on the mechanical response of fire ant rafts. The authors utilized conformational particle image velocimetry (PIV) analysis to obtain the networks' instantaneous velocity field and topological damage responses to elucidate the ant-scale origins of global mechanics. They also spent much effort on elucidating how damage signatures can be explained by the force-induced bond stabilization and quantifying the role of self-healing in mechanical recovery. One main difference from our conclusions is that they did not observe the steady-state creep onset predicted by transient network theory. Perhaps, by incorporating the conformational changes as we did, they will be able to identify the extra plastic behavior between the elastic and rupture regions for a slow pull speed. In addition, we included more properties related to the mechanical response, such as the number of aligned ants vs pull force in Fig. 4 and how it enables us to obtain a partial force structure in Fig. 5, how the length of ant raft relaxes with time under a constant pull force in Fig. 6, and how the effective Young's modulus changes with time during creeping in Fig. 7. In contrast to their focus on the ant scale or the effect of catch bonds between ants, we proposed to treat the ant raft as a group and describe its behavior as emergent properties. We also made heuristic analogies to other physical systems, such as a network of springs in parallel and series. Lastly, the experiments on how the aggregation of ants can be triggered by means other than water and why different species of ants and dead fire ants do not form a raft are also an interesting contribution of our paper.

ACKNOWLEDGMENTS

We are grateful to J. Wang, H. Ko, Khá-Î Tô and J. T. Shy for useful discussions, and to the Department of Economic Development of Hsinchu City Government for supplying the fire ant samples. Financial support from the National Science and Technology Council in Taiwan under Grants No. 111-2112-M007-025 and No. 112-2112-M007-015 is acknowledged.

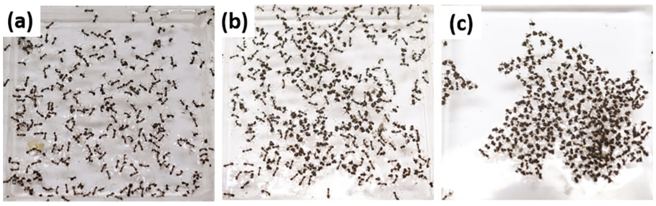

FIG. 9. To test the effect of physiological change of dead ants to raft formation on water, the ratio of freshly dead ants to those of 1-day mortality is modified for roughly 500 dead fire ants. Their ratios are (a) 1:0, (b) 1:1, (c) 0:1.

APPENDIX A: METHOD TO CONTROL THE SIZE OF ANT RAFT

It is tricky to control the length L and width W of an ant raft for reproducibility. The method we developed through trial and error consists of three steps, as described in Fig. 8. Initially, we separate two rods of length W by a distance L. We put roughly 500 fire ants into a beaker. Shaking the beaker will turn the ants into a ball. Then we gently place the ball on the water surface between the rods. The fire ants will gradually spread out and grip the rods. Finally, we use tweezers to trim off the ants that exceed our destined size of W and L. Experience tells us that, if the ants are scattered directly on the water, they can still form the raft, and actually do so faster than if we turn them into a ball first. The problem is that somehow the ants only grip onto the rods very loosely, which made it impossible for the force-displacement experiment.

APPENDIX B: AGGREGATION OF DEAD ANTS

The Cheerios effect has been shown not to be sufficient for the raft formation in Table I by demonstrating that live local ants and dead fire ants do not aggregate on the water. We have argued that the vigorous waving of legs likely leads to repulsion in the former case. But, this explanation apparently does not apply to the dead ants. Then, why is the latter aggregate so porous, compared to that of live ones? The answer to this intriguing mystery turns out to involve some biological facts. When ants are dead less than one day, as is the case in our initial sample, their limbs spread out and tangle up to form an arclike structure that prevents them from getting any closer due to the Cheerios effect, as shown in Fig. 9(a). After exceeding 1-day mortality, this hindrance to aggregate will be mitigated as their legs and bodies, including head, mesosoma, and metasoma, start to curl up into a ball shape. This explanation is supported by the decrease of arc number as we substitute half and all freshly dead ants by 1-day-old ones in Figs. 9(b) and 9(c).

[1] D. J. Pearce, A. M. Miller, G. Rowlands, and M. S. Turner, Proc. Natl. Acad. Sci. USA **111**, 10422 (2014).

[2] W. Bialek, A. Cavagna, I. Giardina, T. Mora, E. Sil-vestri, M. Viale, and A. M. Walczak, Proc. Natl. Acad. Sci. USA **109**, 4786 (2012).

[3] A. Szabó, R. Unnep, E. Méhes, W. Twal, W. Argraves, Y. Cao, and A. Czirók, Phys. Biol. **7**, 046007 (2010).

[4] H. H. Mattingly and T. Emonet, Proc. Natl. Acad. Sci. USA **119**, e2117377119 (2022).

[5] A. Walther and A. H. Muller, Chem. Rev. **113**, 5194 (2013).

[6] J. Elgeti, R. G. Winkler, and G. Gompper, Rep. Prog. Phys. **78**, 056601 (2015).

[7] J. Werfel, K. Petersen, and R. Nagpal, Science **343**, 754 (2014).

[8] T. Sanchez, D. T. Chen, S. J. DeCamp, M. Heymann, and Z. Dogic, Nature (London) **491**, 431 (2012).

[9] M. S. Ascunce, C.-C. Yang, J. Oakey, L. Calcaterra, W.-J. Wu, C.-J. Shih, J. Goudet, K. G. Ross, and D. Shoe-maker, Science **331**, 1066 (2011).

[10] An interesting article listing four unusual and amazing ways that insects team up can be found in https://www.smithsonianmag.com/science-nature/four-unusual-and-amazing-ways-that-insects-team-up-180982911/.

[11] M. Tennenbaum, Z. Liu, D. Hu, and A. Fernandez-Nieves, Nat. Mater. **15**, 54 (2016).

[12] M. Tennenbaum and A. Fernandez-Nieves, Phys. Rev. E **96**, 052601 (2017).

[13] F. J. Vernerey, T. Shen, S. L. Sridhar, and R. J. Wagner, J. R. Soc. Interface **15**, 20180642 (2018).

[14] M. Tennenbaum and A. Fernandez-Nieves, Phys. Rev. E **102**, 012602 (2020).

[15] R. J. Wagner, K. Such, E. Hobbs, and F. J. Vernerey, J. R. Soc. Interface **18**, 20210213 (2021); R. J. Wagner and F. J. Vernerey, PLoS Comput. Biol. **18**, e1009869 (2022).

[16] N. J. Mlot, C. A. Tovey, and D. L. Hu, Proc. Natl. Acad. Sci. USA **108**, 7669 (2011).

[17] H. Ko, M. Hadgu, K. Komilian, and D. L. Hu, Phys. Rev. Fluids **7**, 090501 (2022).

[18] D. Vella and L. Mahadevan, Am. J. Phys. **73**, 817 (2005); A. J. T. M. Mathijssen, M. Lisicki, V. N. Prakash, and E. J. L. Mossige, Rev. Mod. Phys. **95**, 025004 (2023).

[19] J. Lauridsen, G. Chanan, and M. Dennin, Phys. Rev. Lett. **93**, 018303 (2004).

[20] Y. Wang, K. Krishan, and M. Dennin, Phys. Rev. E **73**, 031401 (2006).

[21] M. J. Bowick, L. Giomi, H. Shin, and C. K. Thomas, Phys. Rev. E **77**, 021602 (2008).

[22] M. Twardos and M. Dennin, Phys. Rev. E **71**, 061401 (2005).

[23] H. Ritacco, F. Kiefer, and D. Langevin, Phys. Rev. Lett. **98**, 244501 (2007).

[24] M. Dennin, Phys. Rev. E **70**, 041406 (2004).

[25] J. Lauridsen, M. Twardos, and M. Dennin, Phys. Rev. Lett. **89**, 098303 (2002).

[26] Y. Wang, K. Krishan, and M. Dennin, Phys. Rev. E **74**, 041405 (2006).

[27] C.-C. Kuo and M. Dennin, Phys. Rev. E **87**, 052308 (2013).

[28] G. Q. Xu and M. J. Demkowicz, Phys. Rev. Lett. **111**, 145501 (2013); C. M. Barr, T. Duong, D. C. Bufford, Z. Milne, A. Molkeri, N. M. Heckman, D. P. Adams, A. Srivastava, K. Hattar, M. J. Demkowicz, and B. L. Boyce, Nature (London) **620**, 552 (2023).

[29] G. A. Vliegenthart, A. Ravichandran, M. Ripoll, T. Auth, and G. Gompper, Sci. Adv. **6**, eaaw9975 (2020).

[30] J. Palacci, Science **377**, 710 (2022).

[31] A. Pena-Francesch, H. Jung, M. C. Demirel, and M. Sitti, Nat. Mater. **19**, 1230 (2020).

[32] A. D. Snyder, Z. J. Phillips, J. S. Turicek, C. E. Diesendruck, K. B. Nakshatrala, and Jason F. Patrick, Nat. Commun. **13**, 6511(2022).

[33] C.-H. Li, C. Wang, C. Keplinger, J.-L. Zuo, L. Jin, Y. Sun, P. Zheng, Y. Cao, F. Lissel, C. Linder, X.-Z. You, and Zhenan Bao, Nat. Chem. **8**, 618 (2016).

[34] B. N. J. Persson and E. A. Brener, Phys. Rev. E **71**, 036123 (2005).

[35] M. Fleck, D. Pilipenko, R. Spatschek, and E. A. Brener, Phys. Rev. E **83**, 046213 (2011).

[36] Y. Mulla, G. Oliveri, J. T. B. Overvelde, and G. H. Koenderink, Phys. Rev. Lett. **120**, 268002 (2018).

[37] N. Kayagaki *et al.*, Nature (London) **591**, 131 (2021).

[38] J. Fineberg and M. Marder, Phys. Rep. **313**, 1 (1999).

[39] M. Marder, Nature (London) **381**, 275 (1996).

[40] T. S. Majmudar and R. P. Behringer, Nature (London) **435**, 1079 (2005).

[41] K. E. Daniels, J. E. Kollmer, and J. G. Puckett, Rev. Sci. Instrum. **88**, 051808 (2017).

[42] C. J. Anderson, P. A. Gibson, and A. Fernandez-Nieves, Phys. Rev. E **106**, L012604 (2022).

[43] J. Chen, Insect Sci. **14**, 1 (2007).

[44] S. Guo, M. Gao, X. Xiong, Y. J. Wang, X. Wang, P. Sheng, and P. Tong, Phys. Rev. Lett. **111**, 026101 (2013).

[45] Whether the dead fire ants will aggregate on the water turns out to depend on how long the dead samples are kept. This is dicussed in Appendix B.

[46] *Pheromones and Reproduction in Mammals*, edited by J. Vandenbergh (Academic, New York, 2012), p. 254.

[47] Khá-Î. Tô and S. R. Nagel, Soft Matter **19**, 905 (2023).

[48] J. R. Barber, *Elasticity*, Solid Mechanics and Its Applications Vol. 172, 3rd ed. (Springer, New York, 2010).

[49] See Supplemental Material at http://link.aps.org/supplemental/10.1103/PhysRevE.109.014607 for the videos of a fire ant raft being pulled by an extra slow, slow, or fast speed.

[50] B. Mahanta, A. Tripathy, V. Vishal, T. N. Singh, and P. G. Ranjith, Eng. Geol. **218**, 39 (2017).

[51] See, for instance, https://www.unsw.edu.au/science/our-schools/materials/engage-with-us/high-school-students-and-teachers/online-tutorials/crack-theory/brittle-fracture/ductile-brittle-transition.

[52] An article on the physics of fire ant raft can be found at https://www.colorado.edu/today/2022/03/02/fire-ant-rafts.

[53] R. J. Wagner, S. Lamont, Z. T. White, and F. J. Vernerey, arXiv:2307.11966.